



HAL
open science

New caspase-independent but ROS-dependent apoptosis pathways are targeted in melanoma cells by an iron-containing cytosine analogue

Jeannine C. Franke, Michael Plötz, Aram Prokop, Christoph C. Geilen,
Hans-Günther Schmalz, Jürgen Eberle

► To cite this version:

Jeannine C. Franke, Michael Plötz, Aram Prokop, Christoph C. Geilen, Hans-Günther Schmalz, et al.. New caspase-independent but ROS-dependent apoptosis pathways are targeted in melanoma cells by an iron-containing cytosine analogue. *Biochemical Pharmacology*, 2009, 79 (4), pp.575. 10.1016/j.bcp.2009.09.022 . hal-00544819

HAL Id: hal-00544819

<https://hal.science/hal-00544819>

Submitted on 9 Dec 2010

HAL is a multi-disciplinary open access archive for the deposit and dissemination of scientific research documents, whether they are published or not. The documents may come from teaching and research institutions in France or abroad, or from public or private research centers.

L'archive ouverte pluridisciplinaire **HAL**, est destinée au dépôt et à la diffusion de documents scientifiques de niveau recherche, publiés ou non, émanant des établissements d'enseignement et de recherche français ou étrangers, des laboratoires publics ou privés.

Accepted Manuscript

Title: New caspase-independent but ROS-dependent apoptosis pathways are targeted in melanoma cells by an iron-containing cytosine analogue

Authors: Jeannine C. Franke, Michael Plötz, Aram Prokop, Christoph C. Geilen, Hans-Günther Schmalz, Jürgen Eberle



PII: S0006-2952(09)00801-6
DOI: doi:10.1016/j.bcp.2009.09.022
Reference: BCP 10338

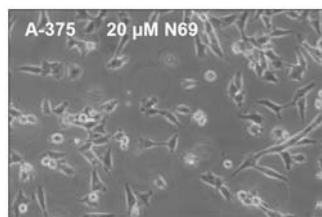
To appear in: *BCP*

Received date: 9-6-2009
Revised date: 6-9-2009
Accepted date: 21-9-2009

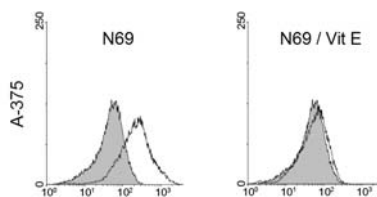
Please cite this article as: Franke JC, Plötz M, Prokop A, Geilen CC, Schmalz H-G, Eberle J, New caspase-independent but ROS-dependent apoptosis pathways are targeted in melanoma cells by an iron-containing cytosine analogue, *Biochemical Pharmacology* (2008), doi:10.1016/j.bcp.2009.09.022

This is a PDF file of an unedited manuscript that has been accepted for publication. As a service to our customers we are providing this early version of the manuscript. The manuscript will undergo copyediting, typesetting, and review of the resulting proof before it is published in its final form. Please note that during the production process errors may be discovered which could affect the content, and all legal disclaimers that apply to the journal pertain.

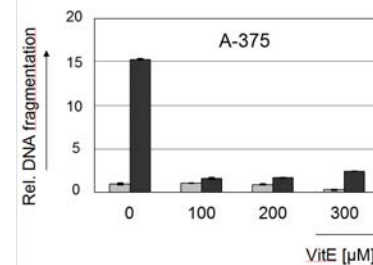
New caspase-independent but ROS-dependent apoptosis pathways are targeted in melanoma cells by an iron-containing cytosine analogue



Induction of apoptosis by N69



Generation of ROS and its inhibition by antioxidant vitamin E



Inhibition of N69-mediated apoptosis by vitamin E

1
2
3 **New caspase-independent but ROS-dependent apoptosis pathways are**
4 **targeted in melanoma cells by an iron-containing cytosine analogue**
5
6
7
8
9

10 **Jeannine C. Franke^{1,2}, Michael Plötz¹, Aram Prokop³, Christoph C. Geilen¹,**

11
12 **Hans-Günther Schmalz⁴ and Jürgen Eberle¹**
13
14
15
16
17
18
19
20

21 ¹ Department of Dermatology and Allergy, Skin Cancer Center Charité, Charitéplatz 1,
22 10117 Berlin, Germany

23
24 ² Free University of Berlin, Department of Biology, Chemistry and Pharmacy, Takustr. 3,
25 14195 Berlin, Germany

26
27
28 ³ University of Cologne, Department of Paediatric Oncology, Amsterdamer Str. 59,
29 50735 Cologne, Germany

30
31 ⁴ University of Cologne, Department of Organic Chemistry, Greinstr. 4,
32 50939 Cologne, Germany
33
34
35
36
37
38
39

40 Correspondence: J. Eberle, PhD

41
42 Charité-Universitätsmedizin Berlin, Department of Dermatology and Allergy, Skin Cancer
43 Center Charité (HTCC), Charitéplatz 1, 10117 Berlin, Germany

44
45 E-mail: juergen.eberle@charite.de
46
47
48
49
50
51
52
53
54

55 Short title: New proapoptotic pathways in melanoma

56
57 Keywords: melanoma; apoptosis; caspase-independent; ROS; Bcl-2; zVAD
58
59

60 Footnote: Aram Prokop and Hans-Günther Schmalz hold a patent on N69
61
62
63
64
65

Abstract

1
2
3
4
5
6
7
8
9
10
11
12
13
14
15
16
17
18
19
20
21
22
23
24
25
26
27
28
29
30
31
32
33
34
35
36
37
38
39
40
41
42
43
44
45
46
47
48
49
50
51
52
53
54
55
56
57
58
59
60
61
62
63
64
65

Chemotherapy resistance and related defects in apoptotic signaling are crucial for the high mortality of melanoma. Effective drugs are lacking, also due to the fact that apoptosis regulation in this tumor is essentially not understood. The cytosine analogue ferroptoside (N69), which contains an iron carbonyl complex, resulted in strong induction of apoptosis in melanoma cells starting already after 2 h, whereas cytotoxicity remained at a low level. Surprisingly, there was no indication for any caspase activation at early times, although cytochrome c was released from mitochondria. Indicative for new proapoptotic pathways was the production of reactive oxygen species (ROS) as an early effect, and the inhibition of apoptosis by the antioxidant vitamin E. Apoptosis was also blocked by exogenous Bcl-2 overexpression and by the pan-protease inhibitor zVAD. However, only zVAD also prevented ROS production, for which Bcl-2 remained without an effect. Thus, new proapoptotic pathways are described here for melanoma cells clearly related to ROS production. A cascade enclosing enhanced levels of intracellular iron, which lead to enhanced ROS production in a Fenton reaction, appears as suggestive. Whereas off-target effects of zVAD appear as upstream, Bcl-2 may exert its inhibitory activity downstream of ROS. New proapoptotic pathways are of particular interest for melanoma as they may open new options for targeting this highly therapy-refractory tumor.

1. Introduction

1
2 Incidence of cutaneous melanoma has dramatically increased in last decades in white
3
4 populations worldwide. Whereas the primary tumor involves the skin, dissemination to
5
6 visceral organs is incurable, with a median survival time of less than 12 months [1;2]. The
7
8 high malignancy is based on a pronounced resistance to conventional chemotherapy, related
9
10 to defects in proapoptotic signaling. Thus, targeting melanoma by efficient induction of
11
12 apoptosis appears as promising [3;4].
13
14
15

16 Two main proapoptotic pathways have been described. The extrinsic pathway is initiated by
17
18 binding of death ligands to cell surface receptors leading to the formation of a death inducing
19
20 signaling complex, where initiator caspases 8 and 10 are activated [5]. In contrast, the
21
22 intrinsic apoptosis pathway is triggered by intracellular signals such as cellular and DNA
23
24 damage, also when caused by chemotherapy. Key events are depolarization of mitochondrial
25
26 membrane potential, mitochondrial outer membrane permeabilisation (MOMP), release of
27
28 mitochondrial cytochrome c into the cytosol, which results in activation of initiator caspase-9
29
30 [3;6;7]. Both pathways may meet at the mitochondria, which are of particular importance in
31
32 apoptosis regulation. Mitochondrial activation is controlled by the family of Bcl-2 proteins,
33
34 which consists of antiapoptotic proteins (e.g. Bcl-2, Bcl-x_L and Mcl-1), proapoptotic
35
36 multidomain proteins (Bax and Bak) and proapoptotic BH3-only proteins (e.g. Bad, Puma and
37
38 Noxa) [8;9]. According to these pathways, caspase cascades appear as central in apoptosis
39
40 regulation. Initiator caspases cleave and activate downstream effector caspases, which
41
42 themselves target a number of death substrates to set apoptosis into work [6;10].
43
44
45
46
47
48
49

50 Besides caspase-dependent apoptosis, several recent reports are strongly suggestive for
51
52 alternative, caspase-independent cell death pathways [11]. Thus, cathepsins have been
53
54 discussed, which may be released from lysosomes into the cytoplasm to contribute to
55
56 apoptosis [12;13]. Furthermore apoptosis-inducing factor (AIF) and endonuclease G,
57
58 frequently found in the cytosol after induction of apoptosis, may trigger DNA fragmentation
59
60
61
62
63
64
65

1 in a caspase-independent way [14]. Finally, reactive oxygen species (ROS) have been
2 discussed in relation to apoptosis control. ROS-mediated damage of membrane proteins and
3 polyunsaturated fatty acids may lead to mitochondrial and lysosomal dysfunction [15;16], and
4 ROS-mediated DNA damage may also result in DNA fragmentation and apoptosis [17;18].
5
6

7
8
9 New drugs are urgently needed for treatment of metastatic melanoma. In nucleoside
10 analogues, different modifications have been realized in approved drugs, and growing interest
11 also arises in the development of organic metal complexes. Metal compounds offer new
12 mechanisms of drug action, which may not be realised by organic residues [19]. Here, we
13 demonstrate the high proapoptotic potential of a recently described iron-containing cytosine
14 analogue ferroptoside (N69, 4g) [20] in human melanoma cells. It appears to target new
15 apoptosis pathways independent of caspase activation but related to the production of ROS.
16
17
18
19
20
21
22
23
24
25
26
27
28
29
30
31
32
33
34
35
36
37
38
39
40
41
42
43
44
45
46
47
48
49
50
51
52
53
54
55
56
57
58
59
60
61
62
63
64
65

2. Materials and methods

2.1. Cell culture

Four human melanoma cell lines were investigated: Mel-HO [21], A-375 [22], Mel-2a [23] and SK-Mel-13 [24]. Subclones of Mel-HO and A-375 resulted from stable transfection of a pIRES-Bcl-2 construct (MelHO-Bcl-2, A375-Bcl-2) or the pIRES empty plasmid (MelHO-Mock, A375-Mock), as previously described [25]. The pIRES plasmid originates from Clontech (Palo Alto, California, USA). Jurkat lymphoma cell line was used as positive control for caspase processing [26]. Melanoma cells were cultured at 37°C, 5% CO₂ in DMEM (4.5 g/l glucose; Gibco, Invitrogen, Karlsruhe, Germany) supplemented with 10% FCS and antibiotics (Biochrom, Berlin, Germany). Experiments were performed in 6-well plates or 24-well plates (200,000 and 50,000 cells/well, respectively). Treatment with N69 [20] was started after 24 h, whereas control cells received only solvent ethanol.

For growth curves, cell confluence was continuously monitored by real-time cell analysis (RTCA, xCELLigence, Roche diagnostics; Penzberg, Germany). The technique is based on microelectrodes integrated in the bottom of each well of special 96-well E-plates. The electric impedance corresponds to the cell density. 10,000 cells were seeded per microtiter well, and treatment started after 24 h. The impedance was determined up to 60 h after seeding with 15 min intervals.

2.2. Quantification of apoptosis and cytotoxicity

For apoptosis quantification, a cell death detection ELISA (Roche Diagnostics, Mannheim, Germany) was used, which detects mono- and oligonucleosomes formed in apoptotic cells. Cytotoxicity was determined in parallel by measuring LDH activity in culture fluids applying a cytotoxicity detection assay (Roche Diagnostics). Protocols were according to the manufacturer with minor modifications [27].

1 Cell cycle analyses were carried out for detection of hypodiploid nuclei [28]. Cells were
2 harvested by trypsinisation, stained with propidium iodide (Sigma, Taufkirchen, Germany;
3
4 200 µg/ml), washed with PBS and analyzed by a FACS Calibur.
5
6

7 For identification of chromatin condensation and nuclear fragmentation in course of
8 apoptosis, cells were harvested by trypsinisation, centrifuged on cytopins and fixed for 30
9 min in 4% formaldehyde. Cytopins were stained with bisbenzimidazole (Hoechst-33258; Sigma,
10 Taufkirchen, Germany; 1µg/ml, 30 min) and examined by fluorescence microscopy.
11
12 Apoptotic cells were identified by fragmented nuclei or by bright blue-stained nuclei with
13 condensed DNA.
14
15

16 Free 3'-OH DNA termini indicating DNA strand breaks in apoptotic cells were labeled by
17 terminal deoxynucleotidyl transferase (TUNEL) using an in situ cell death detection kit
18 (Roche Diagnostics). Cells were harvested by trypsinisation, centrifuged on cytopins and
19 fixed in 4% paraformaldehyde for 1 h. Cytopins were treated with 0.1% Triton-X-100 in
20 sodium citrate buffer and were incubated with TUNEL reaction mix for 1 h at 37°C.
21
22 Apoptotic cells with green nuclei were identified by fluorescence microscopy.
23
24
25
26
27
28
29
30
31
32
33
34
35
36
37
38

39 *2.3. Mitochondrial membrane potential and lysosomal membrane permeabilisation*

40 For determination of mitochondrial membrane potential, the fluorescent dye JC-1 (5,5',6,6'-
41 Tetrachloro-1,1',3,3'-tetraethylbenzimidazolcarbocyanine Iodide) was used. Cells were
42 harvested by trypsinisation, stained with JC-1 (Sigma, Taufkirchen, Germany; 2,5 µM, 15
43 min; 37°C) and analyzed in PBS buffer (Biochrom, Berlin, Germany) by a FACS Calibur.
44
45
46
47
48
49

50 For identification of changes in lysosomal pH, cells were stained with acridine orange. It
51 accumulates in lysosomes to give the typical orange staining under the acidic conditions in
52 intact lysosomes (pH 5). After lysosomal membrane permeabilisation, pH increases according
53 to cytoplasmic conditions (pH 7), and the dye changes from orange to green. Following N69
54 treatment, cells were stained with acridine orange (Sigma, Taufkirchen, Germany; 15 µg/ml,
55
56
57
58
59
60
61
62
63
64
65

1 30 min), harvested by trypsinisation, centrifuged on cytopins and examined by fluorescence
2 microscopy. For time kinetics, cells were harvested by trypsinisation, stained with acridine
3 orange (Sigma, Taufkirchen, Germany; 15 µg/ml, 15 min; 37°C) and suspended in PBS buffer
4 (Biochrom, Berlin, Germany). Green fluorescence was determined by a FACS Calibur.
5
6
7
8
9

10 11 12 2.4. Western blot analysis

13 For caspase analysis, cells were lysed in CHAPS buffer (Cell Signaling, Frankfurt, Germany).
14 For PARP analysis, cells were lysed in 62.5 mM Tris-HCl, pH 6.8; 6 M urea; 10% glycerol;
15 2% SDS; 5% β-mercaptoethanol. For Bcl-2 proteins, cells were lysed in 10 mM Tris-HCl, pH
16 7.5; 150 mM NaCl; 1 mM EDTA; 2 mM PMSF; 1 µM leupeptin; 1 µM pepstatin; 0.5% SDS
17 and 0.5% Nonidet P-40. For cytochrome c and AIF analysis, cytosolic and mitochondrial cell
18 fractions were separated by using a mitochondria/cytosol fractionation kit (Alexis, Grünberg,
19 Germany). For cathepsin analysis, cells were lysed with a tissue grinder in 250 mM sucrose,
20 10 mM Hepes and 1 mM EDTA. Cell lysis was controlled by microscopy. Lysates were
21 centrifuged at 1000 g, and cellular debris were discarded. The supernatant was centrifuged
22 again at 100,000 g for separation of the lysosomal fraction (pellet) and the cytosolic fraction
23 (supernatant).
24
25
26
27
28
29
30
31
32
33
34
35
36
37
38
39
40

41 Protocols for protein extraction and Western blot analysis were described previously [27].

42 The following primary antibodies were used: caspase-2 (Alexis, rat, 1:200), cleaved caspase-3
43 (Cell Signaling, rabbit, 1:1000), caspase-6 (Cell Signaling, rabbit, 1:1000), caspase-7 (Cell
44 Signaling, rabbit, 1:1000), caspase-8 (Cell Signaling, mouse, 1:1000), caspase-9 (Cell
45 Signaling, rabbit, 1:1000), PARP (Biomol, mouse, 1:5000), Mcl-1 (Santa Cruz, mouse,
46 1:200), Bcl-2 (Santa Cruz, mouse, 1:200), Bcl-x_L (Santa Cruz, rabbit, 1:200), Bax (Santa
47 Cruz, rabbit, 1:200), Bak (Dako, rabbit, 1:500), Bad (Cell Signaling, rabbit, 1:1000), Puma
48 (Epitomics, rabbit, 1:1000), Noxa (Pro Sci, rabbit, 1:500), cytochrome c (BD Biosciences,
49 mouse, 1:1000), AIF (Santa Cruz, goat, 1:200), anti-Porin 31 HL (VDAC) (Calbiochem,
50
51
52
53
54
55
56
57
58
59
60
61
62
63
64
65

1 mouse, 1:5000), cathepsine D (Santa Cruz, goat, 1:200), cathepsine L (Santa Cruz, goat,
2 1:200), β -actin (Sigma, mouse, 1:5000) and Hsp-60 (Cayman, mouse, 1:200). The following
3 secondary antibodies were used: peroxidase-labeled anti-rabbit, anti-mouse, anti-goat or anti-
4 rat (Dako, Hamburg, Germany; 1:5000).
5
6
7
8
9

10 2.5. Determination of activated caspase-3 and inhibition of caspases and cathepsins

11 For determination of activated caspase-3, a sandwich ELISA for activated (cleaved) caspase-3
12 was performed (Cell Signaling, Frankfurt, Germany), which detects endogenous levels of
13 cleaved caspase-3 protein. Mel-HO and A-375 cells were incubated with 20 μ M N69 for 6 h
14 and 24 h or were treated with 100 ng CH-11 for 24 h as positive control or were left untreated.
15
16 Cells were preincubated for 1 h with 10 μ M of fluoro-methyl-ketone (fmk)-derivatized
17 oligopeptides, which bind the active sites of caspase-like proteases. The following inhibitors
18 were used: zVAD-fmk (pancaspase/panprotease), zWEHD-fmk (caspase-1), zVDVAD-fmk
19 (caspase-2), zDEVD-fmk (caspase-3), zYVAD-fmk (caspase-4), zVEID-fmk (caspase-6),
20 zIETD-fmk (caspase-8), zLEHD-fmk (caspase-9), zAEVD-fmk (caspase-10) and zLEED-fmk
21 (caspase-13) (R&D Systems, Wiesbaden, Germany).
22
23
24
25
26
27
28
29
30
31
32
33
34
35
36
37
38

39 For inhibition of cathepsins, cells were preincubated for 1 h with different concentrations of
40 fluoro-methyl-ketone (fmk)-derivatized oligopeptides, which bind the active sites of
41 cathepsine-like proteases. The following inhibitors were used: zFA-FMK (cathepsins B, L),
42 CA-074-Me (cathepsin B) (Calbiochem, Germany).
43
44
45
46
47
48
49
50

51 2.7. Determination of ROS

52 For measurement of intracellular ROS levels, the fluorescent dye H₂DCFDA (2',7'-
53 dichlorodihydrofluoresceindiacetate) was used. Cells were stained with H₂DCFDA
54 (Molecular Probes, Invitrogen, Eugene, Oregon, USA; 15 μ M, 30 min), harvested by
55 trypsinisation and analyzed in HBSS buffer (Biochrom, Berlin, Germany) by a FACS Calibur.
56
57
58
59
60
61
62
63
64
65

1 For ROS scavenging, vitamin E (Fluka, Sigma, Steinheim, Germany) was used in different
2 concentrations, starting from a 50 mM stock solution in ethanol. For positive controls, cells
3
4 were treated with H₂O₂ (200 μM; 1h).
5
6
7
8

9 **3. Results**

10 *3.1. Early induction of apoptosis by N69 in melanoma cells*

11
12 The effects of the iron-containing cytosine analogue N69 (Fig 1A) on cell death were
13
14 investigated in four representative human melanoma cell lines (Mel-HO, A-375, Mel-2a and
15
16 SK-Mel-13). Visible effects as reduced cell numbers, rounded cells and cell detachment were
17
18 clearly evident after 24 h (Fig 1B). Induction of apoptosis, as determined after 24 h by DNA-
19
20 fragmentation, was significant at 20 μM (Mel-HO, A-375) and at 30 μM (Mel-2a, SK-Mel-
21
22 13), respectively. Cytotoxicity, determined by LDH-release, was less pronounced at 20 μM
23
24 but was also increased after 24 h treatment with 30 μM N69 (Fig 1C). Investigation of the
25
26 time dependency of N69-induced apoptosis revealed a significant increase already after 2 h in
27
28 Mel-HO and after 5 h in A-375. At these early times, cytotoxicity was unaffected, indicating
29
30 that apoptosis induction was the primary effect (Fig 1D).
31
32
33
34
35
36
37
38

39 Real-time cell analysis (RTCA) was used to determine the effects on cell confluence. Cell
40
41 density of N69-treated A-375 cells was continuously monitored for 60 h in microtiterplates.
42
43 Whereas untreated control cells continuously increased in cell density during this period,
44
45 N69-treated cells showed a dose-dependent and dramatic decrease of cell density, starting at
46
47 6-8 h after N69 was added (Fig 1E).
48
49
50

51 Typical hallmarks of apoptosis were seen in N69-treated Mel-HO and A-375 cells, proving
52
53 the induction of apoptosis. Thus, increased sub-G1 cell populations were evident already at 3
54
55 h after N69 treatment and further increased up to 48 h, indicating apoptotic cells with
56
57 fragmented DNA (Fig 2A). Chromatin condensation, nuclear fragmentation and nuclear
58
59 shrinkage were visualized by bisbenzimidazole staining 48 h after N69 treatment (Fig 2B), and
60
61
62
63
64
65

1 TUNEL staining indicated an increased number of apoptotic cells with free 3'-OH DNA
2 termini at 48 h (Fig 2C). Bisbenzimidazole and TUNEL positivity however appeared as late
3 effects as no significant changes were assessed at 24 h after N69 treatment (data not shown).
4
5 Quantitative evaluations after 48 h revealed largely concordant results for the three assays,
6
7 namely 30% - 50% apoptotic cells upon N69 treatment.
8
9

14 *3.2. N69-induced apoptosis in melanoma cells is independent of caspase activation*

16 For exploring the way of N69-induced apoptosis in melanoma cells, involvement of caspases
17 was investigated by Western blot analysis. However, no processing of any of the
18
19 characteristic proapoptotic caspases (3, 6, 7, 8 or 9) was seen in Mel-HO and A-375 at 6 h or
20
21 at 24 h after 20 μ M N69 treatment. Similarly, no activation of caspase-2 was observed (Fig
22
23 3A). Only after 48 h, typical cleavage products were seen of effector caspase-3 and of the
24
25 caspase-3 target protein poly(ADP-ribose) polymerase (PARP) (Fig 3B). Supporting the
26
27 Western blot data, a highly sensitive sandwich ELISA was performed for the central effector
28
29 caspase-3, which did not reveal any indication for cleaved caspase-3 at 6 h and 24 h after
30
31 treatment (Fig 3C).
32
33

34 The results with selective oligopeptide inhibitors for caspases 1, 2, 3, 4, 6, 8, 9, 10 and 13
35
36 appeared in parallel, as pretreatment for 1 h (10 μ M) remained without effect on the
37
38 proapoptotic activity of N69 (Fig 3C). The inhibitory activity of these substances in
39
40 melanoma cell lines had been demonstrated in a previous study [29]. N69-induced apoptosis
41
42 was however completely abolished by the pancaspase inhibitor zVAD-fmk (Fig 3C), which is
43
44 known to bind a common functional motif of caspases, which is however also shared by other
45
46 proteases [30].
47
48
49
50
51
52
53
54
55
56
57
58
59
60
61
62
63
64
65

3.3. Response of mitochondria but no proapoptotic regulation of Bcl-2 proteins

1
2 Mitochondrial response in apoptosis is associated with decreased mitochondrial membrane
3 potential. A decreased membrane potential was clearly evident after JC-1 staining and FACS
4 analysis in Mel-HO and A-375 cells already at 1 h, 3 h and at 6 h after treatment with 20 μ M
5 N69, again indicating an early apoptotic response (Fig 2B).
6
7

8
9
10
11 Release of mitochondrial factors into the cytosol and translocation of Bax and Bak are
12 hallmarks in the mitochondrial proapoptotic pathway. For evaluating its contribution in N69-
13 mediated apoptosis, mitochondrial and cytosolic fractions were isolated at 3 h, 6 h and 24 h
14 after treatment with 20 μ M N69. Western blot analysis revealed release of cytochrome c and
15 apoptosis inducing factor (AIF) already after 3 h, which further increased with time (Fig 4A).
16
17
18
19
20
21
22
23
24 In parallel, increased levels of Bak but not of Bax were seen in mitochondria (Fig 4B).
25

26
27 Activation of the mitochondrial pathway was however not linked to an upregulation of the
28 expression levels of proapoptotic multidomain Bcl-2-related proteins (Bax, Bak) or
29 proapoptotic BH3-only proteins (Bad, Noxa, Puma), as determined by Western blot analysis
30 in Mel-HO, A-375, Mel-2a and SK-Mel-13 cells at 24 h and 48 h after N69 treatment (20
31 μ M). Rather, upregulation of antiapoptotic Mcl-1 (Mel-HO, Mel-2a, SK-Mel-13) and Bcl-x_L
32 (A-375, Mel-2a, SK-Mel-13) was found in an antiapoptotic response (Fig 4D).
33
34
35
36
37
38
39
40

41
42 In addition, we investigated the expression of the transcription factor and apoptosis inducer
43 p53, which has been reported to drive the expression of several proapoptotic Bcl-2 proteins as
44 Bax, Puma and Noxa. Expression of p53 appeared as strongly enhanced in course of N69
45 treatment in the melanoma cell lines A-375, Mel-2a and SK-Mel-13, but was not regulated in
46 Mel-HO. However, there was no correlation between upregulation of p53 and expression of
47 indicated proapoptotic Bcl-2 proteins.
48
49
50
51
52
53
54
55
56
57
58
59
60
61
62
63
64
65

3.4. Involvement of lysosomes

1
2 Lysosomal membrane permeabilisation was investigated by staining with acridine orange
3 (AO). Untreated Mel-HO and A-375 cells revealed typical orange staining indicating intact
4 lysosomes, whereas treatment with N69 (20 μ M; 48 h) resulted in a characteristic green
5 staining of about 60% of Mel-HO and A-375 cells, indicating lysosomal involvement (Fig
6 2D). These changes to green were determined by FACS analysis for Mel-HO and A-375 cells
7 in a time kinetic at 1 h, 3 h, 6 h and 24 h after treatment with N69. Significant increases in
8 green fluorescence were observed already at 1 h after N69 treatment, which further increased
9 with time, thus proving changes at the lysosomal membranes as associated with early
10 apoptosis effects (Fig 2E).

11
12 Release of lysosomal proteases has been discussed as contributing to apoptosis induction.
13 Also, cathepsin D and L showed some increase in their cytosolic levels after N69 treatment,
14 indicating lysosomal release of cathepsins in course of N69-mediated apoptosis. This release
15 however occurred only lately, after 48 h, likely characterizing the possible involvement of
16 cathepsins as secondary in N69-mediated apoptosis (Fig 4C). Largely in agreement, the pre-
17 treatment of melanoma cells with the cathepsin inhibitors zFA-FMK and CA-074-Me (1 h, 5-
18 20 μ M) was not able to prevent N69-induced apoptosis (Fig 3E; 3F). The use of higher
19 concentrations of these inhibitors induced apoptosis itself in melanoma cells (data not shown).

3.5. Association of N69-mediated apoptosis and ROS production

20
21 Intracellular iron may result in production of ROS. Indeed, significantly increased ROS levels
22 were detected by FACS analysis after H₂DCFDA staining in Mel-HO and A-375 cells at 1 h,
23 3 h and at 6 h after treatment with 20 μ M N69 (Fig 5A). The role of ROS in N69-induced
24 apoptosis was further investigated by application of the lipophilic antioxidant vitamin E
25 (VitE). Pretreatment for 1 h with VitE was able to block N69-mediated ROS production (Fig
26 5B) and also almost completely abolished N69-induced apoptosis (Fig 5C).

3.6. ROS production is blocked by the panprotease inhibitor zVAD but not by Bcl-2

For better understanding the steps involved in N69-mediated apoptosis in melanoma cells, the effects of characteristic antiapoptotic agents, namely ectopic overexpression of Bcl-2 and the pancaspase/panprotease inhibitor zVAD were investigated. Subclones of Mel-HO and A-375, stably transfected with a Bcl-2 expression plasmid were completely protected from the proapoptotic effects of N69, as compared to mock-transfected cells (Fig 6A). Similarly, pretreatment with zVAD was able to completely prevent N69-induced apoptosis in both cell lines (Fig 3C). However, whereas Bcl-2 overexpression was without an effect on ROS levels indicating its antiapoptotic activity downstream of ROS (Fig 6B), zVAD also prevented N69-induced ROS production thus indicative for upstream targets (Fig 6C).

4. Discussion

Induction of apoptosis by intrinsic pathways appears as a critical issue in cancer therapy [4]. For metastatic melanoma however, chemotherapies were not effective so far and are even not able to extend life expectancy of patients [2]. This may be seen as an indication that described intrinsic apoptosis pathways may not be the suitable target in melanoma [31]. Nevertheless, apoptosis is induced in melanoma cells in vitro by strategies such as overexpression of proapoptotic Bcl-2 proteins [31], but these investigations had suggested a predominance of caspase-independent pathways [29;32].

New drugs may have the chance to overcome melanoma therapy resistance, when such alternative pathways are targeted. Organometallic nucleoside analogues are new candidates [19], and for the iron-containing nucleoside analogue ferroptoside (N69), proapoptotic activity has previously been demonstrated in a lymphoma cell line [20]. Here, we show strong and early induction of apoptosis by N69 in melanoma cells, as proven by independent

1 apoptosis assays which are largely in agreement with recent recommendations for the
2 classification of cell death [33]. In contrast, cytotoxicity appeared as a secondary effect.
3

4 However, N69-mediated apoptosis in melanoma cells appeared as distinct from previously
5 described signal transduction pathways. Caspases were clearly not involved in the initial
6 phase and were activated only lately due to cellular amplification loops. In contrast,
7 production of ROS appeared as an early effect, and ROS scavenging by the lipophilic
8 antioxidant vitamin E completely abolished N69-mediated apoptosis. The antioxidative
9 activity of vitamin E had previously been demonstrated in other cellular models [34;35].
10

11 ROS are involved in the regulation of different signal transduction pathways including MAP
12 kinases and transcription factors [15], and ROS have also been discussed as contributing to
13 the regulation of apoptosis [36-38]. The mitochondrial respiratory chain is the major source of
14 intracellular ROS, which results in generation of the superoxide anion as the predominant
15 precursor, and in subsequent H_2O_2 production by superoxide dismutase [37]. When
16 interacting with H_2O_2 , intracellular iron may trigger the generation of the highly reactive
17 hydroxyl radical in a Fenton reaction [39;40]. Thus, N69-mediated ROS production may
18 result from its capacity as an iron donor, and the nucleoside structure may exert a carrier
19 function.
20

21 Different mechanisms have been suggested how ROS may lead to apoptosis and DNA
22 fragmentation, These are again mainly based on caspase activation [37]. Production of ROS
23 has clearly been related to DNA damage, particularly described in skin cells after UV-
24 irradiation. ROS causes different kinds of DNA damage as purine and pyrimidine
25 modification, DNA protein crosslinks, backbone damage and strand breaks [17;18]. One
26 might then expect a classical DNA damage response involving p53 activation, enhanced
27 expression of proapoptotic Bcl-2 proteins and downstream mitochondrial and caspase-
28 9/caspase-3 activation [6]. Cytochrome c mobilization and thus its release are also facilitated
29 through ROS-mediated oxidative modification of cardiolipin. Cytochrome c is linked to the
30
31
32
33
34
35
36
37
38
39
40
41
42
43
44
45
46
47
48
49
50
51
52
53
54
55
56
57
58
59
60
61
62
63
64
65

1 inner mitochondrial membrane through cardiolipin, and mitochondrial membrane proteins and
2 lipids are primary targets of ROS [15;37].
3

4
5 In agreement with a DNA damage response, we found enhanced p53 levels in three of the
6 melanoma cell lines. Also, mitochondria were activated early in N69-induced apoptosis in
7 melanoma cells, as shown by decreased membrane potential, release of cytochrome c and
8 enhanced Bak levels in mitochondria. Bak is considered as mitochondrial protein, which
9 deeper integrates into the mitochondrial membrane upon induction of apoptosis. The higher
10 levels that we observed in mitochondria may indicate that the used extraction protocol
11 distinguishes between strong and loose association. Enhanced Bak levels in mitochondria were
12 also seen in glioblastoma cells after treatment with a NO donor [41] and in hepatoma cells
13 treated with the natural flavonoid luteolin [42].
14
15
16
17
18
19
20
21
22
23
24
25
26

27 Thus parts of a DNA damage response appear as activated in melanoma cells by N69.
28
29 However, apoptosis control in melanoma often looks different. Thus, the role of p53 in
30 melanoma is not clear, and the p53 pathway is believed to be blocked despite the lack of
31 inactivating mutations [31]. In agreement, there was no correlation between p53 upregulation
32 by N69 and the expression of known p53 targets in the Bcl-2 family as Bax, Noxa and Puma
33 [43]. As there was no indication for any downstream caspase cascade in case of N69 in
34 melanoma cells, the described effects of N69 at the mitochondria may lead to a dead end as
35 much as the caspases are concerned. The role of p53 in N69-mediated apoptosis may rather be
36 related to regulation of ROS, as also several REDOX genes have been described as p53
37 targets [43].
38
39
40
41
42
43
44
45
46
47
48
49
50

51 ROS-dependent but caspase-independent apoptosis has been reported in several cell models,
52 as in fibroblasts after treatment with cadmium or curcumin [44;45], in cervical cancer cells
53 treated with arsenic trioxide [46] and in squamous cell carcinoma cells treated with cisplatin
54 [47]. The precise pathways however remained elusive and have been partly explained by the
55 mitochondrial release of AIF and endonuclease G. Melanoma cells revealed relatively high
56
57
58
59
60
61
62
63
64
65

1 cytoplasmic AIF levels already before treatment, which were enhanced by N69. Given its
2 activity to mediate caspase-independent DNA fragmentation [14], AIF may have an
3 additional contribution in N69-mediated apoptosis.
4
5

6 Also lysosomes and lysosomal release of proteases such as cathepsins have been discussed as
7 inductors of apoptosis either upstream or independent of caspases [12]. Significant lysosomal
8 changes were detected after N69 treatment in melanoma cells, which appeared at early times
9 in parallel to apoptosis induction. However, a cathepsin release was seen only at later times,
10 and cathepsin inhibitors were not able to prevent early N69-induced apoptosis. Cathepsins
11 may thus contribute to the late phase of N69-mediated apoptosis rather than being involved in
12 its early caspase-independent effects.
13
14
15
16
17
18
19
20
21
22

23 The apoptosis pathways activated by N69 in melanoma cells were further illuminated by
24 investigation of the antiapoptotic activities of zVAD and Bcl-2. The pancaspase inhibitor
25 zVAD has already been shown to exert several other activities as a general inhibition of
26 cysteine proteases including cathepsins, papain and legumain [30]. A relation between z-VAD
27 and ROS generation has been already suggested for betulinic acid-induced cell death in
28 prostate cancer cells, where z-VAD-fmk reduced ROS generation as well as DNA
29 fragmentation [48]. We had parallel findings in melanoma cells, namely inhibition of N69-
30 mediated ROS production and inhibition of apoptosis by zVAD. The nature of zVAD targets
31 upstream of ROS however remains unclear both for prostate cancer and for melanoma cells.
32
33
34
35
36
37
38
39
40
41
42
43
44

45 Antiapoptotic Bcl-2-related proteins suppress the activities of Bax, Bak and BH3-only
46 proteins and thus prevent MOMP and cytochrome c release [7]. It was speculated that they
47 may also be enrolled in control of mitochondrial ROS generation [15;46]. In several studies
48 Bcl-2 overexpression was shown to protect from ROS insults, which was related to enhances
49 activities of antioxidant molecules such as superoxide dismutase and glutathione after Bcl-2
50 overexpression [49;50]. In melanoma cells, ectopic Bcl-2 overexpression efficiently blocked
51
52
53
54
55
56
57
58
59
60
61
62
63
64
65

1 N69-induced apoptosis, however was without effect on the generation of ROS, thus indicating
2 that Bcl-2 exerts its antiapoptotic activities downstream of primary ROS generation.
3

4 Also antiapoptotic changes were observed at the level of the Bcl-2 proteins after N69
5 treatment, as upregulation of Mcl-1 and Bcl-x_L. These proteins were also upregulated in
6 melanoma cells after treatment with the proteasome inhibitor bortezomib [51]. Such
7 counterregulations may diminish the proapoptotic efficacy of drugs, and strategies for
8 targeting antiapoptotic Bcl-2 proteins, such as by BH3 mimetics [31], might be helpful to
9 further enhance also N69-mediated apoptosis.
10
11

12 The existence of new apoptosis pathways in melanoma cells is demonstrated in the present
13 study. A cascade enclosing intracellular iron, which leads to enhanced ROS production in a
14 Fenton reaction, appears as suggestive. Whether these pathways are only targeted by the drug
15 used here, or whether they are of general importance for melanoma and have been overlooked
16 so far, needs further clarification. New targets may arise with the new pathways addressed
17 here. There is the hope that an Achilles' heal of melanoma may be exposed leading to new
18 treatment options for this highly therapy-refractory tumor.
19
20
21
22
23
24
25
26
27
28
29
30
31
32
33
34
35
36
37
38

39 **Acknowledgments**

40
41 The study was supported by research grants from the Charité – Universitätsmedizin Berlin
42
43
44
45
46
47
48
49
50
51
52
53
54
55
56
57
58
59
60
61
62
63
64
65

Figure legends

Fig 1 – Dose and time-dependent induction of apoptosis by N69 in melanoma cells

A) Chemical structure of the iron-containing cytosine analogue N69 (TDS = thexyldimethylsilyl). B) Example of A-375 cells treated for 24 h with 20 μ M N69. Detached and rounded cells are indicative for cell death. C) Dose-dependent DNA-fragmentation indicating apoptosis (upper panel) and LDH-release indicating cytotoxicity (lower panel) are shown for four melanoma cell lines at 24 h after N69 treatment. Concentrations were varied from 10 μ M to 25 μ M for highly sensitive cells (Mel-HO, A-375) and from 20 μ M to 35 μ M for moderate sensitive cells (Mel-2a, SK-Mel-13). The data of Fig 1C and 1D represent relative fragmentation values (fold changes versus untreated controls). Values of untreated cells were set to 1. Bars represent mean values \pm SD of a representative of three independent experiments, each experiment consisting of triple values. Independent experiments revealed comparable results. D) Time-dependent DNA-fragmentation and LDH-release are shown for Mel-HO and A-375 treated with 20 μ M N69. Each time had its own control (not shown), and the values were normalized according the respective controls (C, set to 1). Bars represent mean values \pm SD of a representative of two independent experiments, each consisting of triple values. Independent experiments revealed comparable results. E) Real-time cell analysis (RTCA) is shown for A-375 cells treated with 10, 20 and 30 μ M N69. Seeding density was 10,000 cells per microtiter well. Treatment started at 24 h, and monitoring was for 60 h. The determined cell index gives a relative measurement of cell numbers. The experiment was performed three times, each time triple values, which revealed comparable results.

Fig 2 – Hallmarks of apoptosis after N69 treatment

A) Increased sub-G1 cell populations were determined by FACS analysis after PI staining for Mel-HO and A-375 treated with 20 μ M N69 for 3 h, 6 h, 16 h 24 h and 48 h. Left side:

1 examples are shown of control cells (C), cells treated for 6 h and cells treated for 24 h with
2 N69. Right side: quantification is shown of all times determined. Means and SDs of triple
3 values in a representative experiment are shown. The whole experiment was repeated once.
4

5
6
7 B) Chromatin condensation and nuclear fragmentation were visualized by bisbenzimidazole
8 (DAPI) staining after N69 treatment (20 μ M; 48 h).
9

10
11
12 C) DNA strand breaks were visualized by TUNEL staining after N69 treatment (20 μ M; 48
13 h).
14

15
16 D) Increased acridine orange (AO) staining after N69 treatment (20 μ M, 48 h) is visualized by
17 fluorescence microscopy. A change from orange to green reflects an increased lysosomal pH.
18

19
20 A-D) Quantitative evaluations are shown on the right side. Bars represent percentages of
21 positive cells (mean values \pm SD of triplicate determinations). All experiments were
22 repeated once, which revealed comparable results.
23

24
25
26 E) Green fluorescence after acridine orange staining was determined by FACS analysis.
27 Increased levels are shown in Mel-HO and A-375 cells treated for 1 h, 3 h, 6 h and 24 h with
28 20 μ M N69 (red line, open graphs). Treated cells were compared to non-treated controls
29 (grey). The whole experiment has been repeated once, which revealed comparable results.
30
31
32
33
34
35
36
37
38
39
40

41 **Fig 3 – No early caspase activation by N69**

42
43 A) Proteins were extracted from Mel-HO and A-375 cells after treatment with N69 (20 μ M, 6
44 h and 24 h, as indicated). Described cleavage products of caspases, indicated by a ✂, were
45 seen only in the positive control (C = doxorubicin-treated Jurkat cells). The illustrated
46 Western blots of N69-treated cells correspond to long-term exposures to X-Ray films.
47
48
49
50
51
52
53
54
55
56
57
58
59
60
61
62
63
64
65
Molecular weights are indicated in kDa. N.s. indicates a non specified band seen in melanoma
cells with the caspase-6 antibody.

1 B) Caspase-3 and PARP cleavage monitored at 6 h, 24 h and 48 h after N69 treatment
2 demonstrate late activation (48 h). Analysis for β -actin (A and B) demonstrates equal protein
3 loading (50 μ g/lane). Experiments were repeated twice, which revealed comparable results.
4

5
6
7 C) Activated Caspase-3 was determined by ELISA. Mel-HO and A-375 cells were incubated
8 with 20 μ M N69 for 6 h and 24 h and were compared to non-treated controls kept for the
9 same time (C), set to 1. As positive controls, cells were treated with 100 ng CH-11 agonistic
10 CD95 antibody for 24 h (CH-11). The determinations have been performed 4-times (two
11 independent experiment). Means and SDs of all four values are shown.
12
13
14
15
16
17
18

19 D) Relative DNA fragmentation values (apoptosis) are shown of Mel-HO and A-375 cells
20 treated for 24 h with 20 μ M N69 alone (N) as compared to untreated control cells (C). Parallel
21 cultures were preincubated for 1 h before N69 treatment with the pancaspase inhibitor zVAD-
22 fmk (ZV) or with 10 μ M of selective peptide inhibitors for caspases 1, 2, 3, 4, 6, 8, 9, 10 and
23 13 (C1-C13). For each inhibitor, an individual control without N69 was determined, and each
24 value was normalized according to its own control, which had been set to 1 (not shown). Bars
25 represent mean values \pm SD of one representative of two independent experiments. Both
26 experiments consisted of triple values and revealed comparable results.
27
28
29
30
31
32
33
34
35
36
37

38 E, F) Relative DNA fragmentation values (apoptosis), as determined by ELISA, are shown for
39 Mel-HO and A-375 cells pretreated for 1 h with increasing concentrations (0, 5, 10, 20 μ M)
40 of cathepsin inhibitors z-FA (E) and CA-074 (F). Cells were treated for 24 h with 20 μ M of
41 N69 (dark bars), and apoptosis was compared to control cultures without N69 (C, light grey).
42
43
44
45
46
47
48
49
50
51
52
53
54
55
56
57
58
59
60
61
62
63
64
65

Values were normalized to completely untreated cells, set to 1. Bars represent mean values \pm SD of a representative of two independent experiments. Both experiments consisted of triple values and revealed comparable results.

Fig 4 – Response of mitochondria and Bcl-2 proteins

1
2 A) Decreased mitochondrial membrane potential, as determined by FACS analysis after JC-1
3 staining, is shown for Mel-HO and A-375 treated for 1 h, 3 h and 6 h with 20 μ M N69 (open
4 graph) as compared to non-treated controls (grey). The whole experiment has been repeated
5
6
7
8
9
10 once, which revealed comparable results.

11 B) Mitochondrial fractions (Mito) and cytosolic fractions (Cyto) were isolated of Mel-HO and
12
13 A-375 cells treated with 20 μ M N69 for 3 h, 6 h and 24 h. Cytosolic extracts were analyzed
14
15
16 by Western blotting for the release of cytochrome c and AIF. Treated cells were compared to
17
18 untreated controls kept for 24 h in parallel (C). Mitochondrial extracts were loaded as
19
20 additional controls, and analysis of the mitochondrial protein VDAC ruled out any
21
22 contamination of cytosolic extracts with mitochondria. Beta-actin served as the cytosolic
23
24 loading control (20 μ g/lane).
25
26
27

28 C) Mitochondrial extracts of N69-treated Mel-HO and A-375 cells were analysed for
29
30 translocation of Bax or Bak. Untreated cells were kept in parallel for 24 h (C). Heat shock
31
32 protein 60 (Hsp-60) showed equal loading of mitochondrial extracts (20 μ g/lane).
33
34
35 Experiments (B/C) were repeated once, which revealed comparable results.
36
37

38 D) Cytosolic extracts of Mel-HO and A-375 treated with N69 (20 μ M; 12 h, 24 h and 48 h)
39
40 were analyzed for release of cathepsin D and L. Untreated controls were kept for 48 h in
41
42 parallel (C). Lysosomal extracts were loaded as positive controls. Beta-actin served as the
43
44 cytosolic loading control (50 μ g/lane). The experiment was repeated twice, which revealed
45
46
47 comparable results.
48
49

50 E) Antiapoptotic Bcl-2 proteins (Mcl-1, Bcl-2, Bcl-x_L), proapoptotic multidomain Bcl-2
51
52 proteins (Bax, Bak), propoptotic BH3-only Bcl-2 proteins (Bad, Puma, Noxa) and p53 were
53
54 investigated by Western blot analysis. Their expression was determined in four melanoma cell
55
56 lines treated for 24 h and 48 h with 20 μ M N69 and compared to untreated controls (C). Beta-
57
58
59

1
2
3
4
5
6
7
8
9
10
11
12
13
14
15
16
17
18
19
20
21
22
23
24
25
26
27
28
29
30
31
32
33
34
35
36
37
38
39
40
41
42
43
44
45
46
47
48
49
50
51
52
53
54
55
56
57
58
59
60
61
62
63
64
65

actin served as loading control (50 µg/lane). Experiments were repeated once, which revealed comparable results.

Fig 5 – Involvement of ROS in N69-mediated apoptosis

A) ROS levels were determined by H₂DCFDA staining and FACS analysis in Mel-HO and A-375 cells at 1 h, 3 h and 6 h after N69 treatment (open graphs) and were compared to untreated controls (grey). H₂O₂-treated cells (200 mM; 1 h) served as positive controls. A shift to higher fluorescence corresponds to increased ROS levels. Experiments were repeated twice, which revealed comparable results. B) A-375 cells were pretreated for 1 h with 200 µM vitamin E (VitE) before N69 was given (20 µM; 24 h). N69-treated cells (open graphs) were compared to cells without N69 (grey). Experiments were repeated twice, which revealed comparable results. C) Apoptosis rates are shown for A-375 and Mel-HO cells pretreated for 1 h with increasing concentrations (100-300 µM) of vitamin E (VitE) before N69 treatment (20 µM; 24 h). Comparison was performed to non pretreated cells (0 µM VitE; 20 µM N69, 24 h). Relative DNA-fragmentation rates are shown with respect to untreated controls. Bars represent mean values +/- SD of a representative of two independent experiments, each consisting of triple values. Independent experiments revealed comparable results.

Fig 6 – Effects of Bcl-2 and zVAD on ROS production

A) Cell clones of Mel-HO and A-375 stably transfected with a Bcl-2-pIRES expression construct (Bcl-2) and pIRES-transfected control clones (Mock) were treated with N69 (20 µM; 24 h). Relative apoptosis and cytotoxicity values were calculated with respect to untreated Mock cells (set to 1). Bars represent mean values +/- SD of a representative of three independent experiments, each consisting of triple values. Independent experiments revealed comparable results. B) ROS levels were determined in a cell clone of A-375 stably transfected with a Bcl-2-pIRES expression construct (Bcl-2) and in a pIRES-transfected control clone

1 (Mock). Cells were treated with N69 (20 μ M; 1 h and 24 h; open graphs) and compared to
2 untreated controls (grey). The experiment was repeated twice, which revealed comparable
3 results. C) ROS levels were determined in A375 cells after N69 treatment (20 μ M; 1 and 24 h;
4 open graphs) and compared to untreated controls (grey). In addition, cells received
5 pretreatment with zVAD (10 μ M; 1 h, right side). Cultures without zVAD are shown on the
6 left side. The experiment was repeated twice, which revealed comparable results.
7
8
9
10
11
12
13
14
15
16
17
18
19
20
21
22
23
24
25
26
27
28
29
30
31
32
33
34
35
36
37
38
39
40
41
42
43
44
45
46
47
48
49
50
51
52
53
54
55
56
57
58
59
60
61
62
63
64
65

Reference List

1. Balch CM, Buzaid AC, Soong SJ, Atkins MB, Cascinelli N, Coit DG, Fleming ID, Gershenwald JE, Houghton A, Kirkwood JM, McMasters KM, Mihm MF, Morton DL, Reintgen DS, Ross MI, Sober A, Thompson JA, and Thompson JF, Final version of the American Joint Committee on Cancer staging system for cutaneous melanoma. *Journal of Clinical Oncology* 19: 3635-3648, 2001.
2. Garbe C, Hauschild A, Volkenandt M, Schadendorf D, Stolz W, Reinhold U, Kortmann RD, Kettelhack C, Frerich B, Keilholz U, Dummer R, Sebastian G, Tilgen W, Schuler G, Mackensen A, and Kaufmann R, Evidence and interdisciplinary consensus-based German guidelines: diagnosis and surveillance of melanoma. *Melanoma Res.* 17: 393-399, 2007.
3. Soengas MS and Lowe SW, Apoptosis and melanoma chemoresistance. *Oncogene* 22: 3138-3151, 2003.
4. Eberle J, Fecker LF, Forschner T, Ulrich C, Rowert-Huber J, and Stockfleth E, Apoptosis pathways as promising targets for skin cancer therapy. *British Journal of Dermatology* 156: 18-24, 2007.
5. Krammer PH, Arnold R, and Lavrik IN, Life and death in peripheral T cells. *Nat.Rev.Immunol.* 7: 532-542, 2007.
6. Riedl SJ and Shi Y, Molecular mechanisms of caspase regulation during apoptosis. *Nat.Rev.Mol.Cell Biol.* 5: 897-907, 2004.
7. Chipuk JE and Green DR, How do BCL-2 proteins induce mitochondrial outer membrane permeabilization? *Trends Cell Biol.* 18: 157-164, 2008.
8. Daniel PT, Schulze-Osthoff K, Belka C, and Guner D, Guardians of cell death: the Bcl-2 family proteins. *Essays Biochem.* 39: 73-88, 2003.
9. Hossini AM and Eberle J, Apoptosis induction by Bcl-2 proteins independent of the BH3 domain. *Biochemical Pharmacology*, 2008.
10. Los M, Stroh C, Janicke RU, Engels IH, and Schulze-Osthoff K, Caspases: more than just killers? *Trends Immunol.* 22: 31-34, 2001.
11. Tait SW and Green DR, Caspase-independent cell death: leaving the set without the final cut. *Oncogene* 27: 6452-6461, 2008.
12. Chwieralski CE, Welte T, and Buhling F, Cathepsin-regulated apoptosis. *Apoptosis.* 11: 143-149, 2006.
13. Broker LE, Kruyt FAE, and Giaccone G, Cell death independent of caspases: A review. *Clinical Cancer Research* 11: 3155-3162, 2005.
14. Lorenzo HK and Susin SA, Therapeutic potential of AIF-mediated caspase-independent programmed cell death. *Drug Resist.Updat.* 10: 235-255, 2007.
15. Fleury C, Mignotte B, and Vayssiere JL, Mitochondrial reactive oxygen species in cell death signaling. *Biochimie* 84: 131-141, 2002.

16. Lockshin RA and Zakeri Z, Apoptosis, autophagy, and more. *International Journal of Biochemistry & Cell Biology* 36: 2405-2419, 2004.
17. Dizdaroglu M, Jaruga P, Birincioglu M, and Rodriguez H, Free radical-induced damage to DNA: mechanisms and measurement. *Free Radic.Biol.Med.* 32: 1102-1115, 2002.
18. Pelicano H, Carney D, and Huang P, ROS stress in cancer cells and therapeutic implications. *Drug Resist.Updat.* 7: 97-110, 2004.
19. Ott I and Gust R, Non platinum metal complexes as anti-cancer drugs. *Arch.Pharm.(Weinheim)* 340: 117-126, 2007.
20. Schlawe D, Majdalani A, Velcicky J, Hessler E, Wieder T, Prokop A, and Schmalz HG, Iron-containing nucleoside analogues with pronounced apoptosis-inducing activity. *Angew.Chem.Int.Ed Engl.* 43: 1731-1734, 2004.
21. Holzmann B, Lehmann JM, Zieglerheitbrock HWL, Funke I, and Riethmuller G, Glycoprotein P3.58, Associated with Tumor Progression in Malignant-Melanoma, Is A Novel Leukocyte Activation Antigen. *International Journal of Cancer* 41: 542-547, 1988.
22. Giard DJ, Aaronson SA, Todaro GJ, Arnstein P, Kersey JH, Dosik H, and Parks WP, In-Vitro Cultivation of Human Tumors - Establishment of Cell Lines Derived from A Series of Solid Tumors. *Journal of the National Cancer Institute* 51: 1417-1423, 1973.
23. Bruggen J, Sorg C, and Macher E, Membrane-Associated Antigens of Human Malignant Melanoma-V - Serological Typing of Cell Lines Using Antisera from Nonhuman-Primates. *Cancer Immunology Immunotherapy* 5: 53-62, 1978.
24. Carey TE, Takahashi T, Resnick LA, Oettgen HF, and Old LJ, Cell-Surface Antigens of Human Malignant-Melanoma - Mixed Hemadsorption Assays for Humoral Immunity to Cultured Autologous Melanoma Cells. *Proceedings of the National Academy of Sciences of the United States of America* 73: 3278-3282, 1976.
25. Raisova M, Hossini AM, Eberle J, Riebeling C, Wieder T, Sturm I, Daniel PT, Orfanos CE, and Geilen CC, The Bax/Bcl-2 ratio determines the susceptibility of human melanoma cells to CD95/Fas-mediated apoptosis. *J.Invest Dermatol.* 117: 333-340, 2001.
26. Schneider U, Schwenk HU, and Bornkamm G, Characterization of Ebv-Genome Negative Null and T-Cell Lines Derived from Children with Acute Lymphoblastic Leukemia and Leukemic Transformed Non-Hodgkin Lymphoma. *International Journal of Cancer* 19: 621-626, 1977.
27. Eberle J, Fecker LF, Hossini AM, Wieder T, Daniel PT, Orfanos CE, and Geilen CC, CD95/Fas signaling in human melanoma cells: conditional expression of CD95L/FasL overcomes the intrinsic apoptosis resistance of malignant melanoma and inhibits growth and progression of human melanoma xenotransplants. *Oncogene* 22: 9131-9141, 2003.

- 1 28. Nicoletti I, Migliorati G, Pagliacci MC, Grignani F, and Riccardi C, A Rapid and
2 Simple Method for Measuring Thymocyte Apoptosis by Propidium Iodide Staining
3 and Flow-Cytometry. *Journal of Immunological Methods* 139: 271-279, 1991.
- 4 29. Oppermann M, Geilen CC, Fecker LF, Gillissen B, Daniel PT, and Eberle J, Caspase-
5 independent induction of apoptosis in human melanoma cells by the proapoptotic Bcl-
6 2-related protein Nbk / Bik. *Oncogene*. 24: 7369-7380, 2005.
- 7 30. Rozman-Pungercar J, Kopitar-Jerala N, Bogyo M, Turk D, Vasiljeva O, Stefe I,
8 Vandenamee P, Bromme D, Puizdar V, Fonovic M, Trstenjak-Prebanda M, Dolenc I,
9 Turk V, and Turk B, Inhibition of papain-like cysteine proteases and legumain by
10 caspase-specific inhibitors: when reaction mechanism is more important than
11 specificity. *Cell Death.Differ.* 10: 881-888, 2003.
- 12 31. Eberle J, Kurbanov BM, Hossini AM, Trefter U, and Fecker LF, Overcoming
13 apoptosis deficiency of melanoma - Hope for new therapeutic approaches. *Drug*
14 *Resistance Updates* 10: 218-234, 2007.
- 15 32. Hossini AM, Geilen CC, Fecker LF, Daniel PT, and Eberle J, A novel Bcl-x splice
16 product, Bcl-x(AK), triggers apoptosis in human melanoma cells without BH3
17 domain. *Oncogene*. : 2005.
- 18 33. Kroemer G, Galluzzi L, Vandenamee P, Abrams J, Alnemri ES, Baehrecke EH,
19 Blagosklonny MV, El-Deiry WS, Golstein P, Green DR, Hengartner M, Knight RA,
20 Kumar S, Lipton SA, Malorni W, Nunez G, Peter ME, Tschopp J, Yuan J, Piacentini
21 M, Zhivotovsky B, and Melino G, Classification of cell death: recommendations of the
22 Nomenclature Committee on Cell Death 2009. *Cell Death.Differ.* 16: 3-11, 2009.
- 23 34. Wu SJ, Ng LT, and Lin CC, Effects of vitamin E on the cinnamaldehyde-induced
24 apoptotic mechanism in human PLC/PRF/5 cells. *Clinical and Experimental*
25 *Pharmacology and Physiology* 31: 770-776, 2004.
- 26 35. Gopal DVR, Narkar AA, Badrinath Y, Mishra KP, and Joshi DS, Protection of
27 Ewing's sarcoma family tumor (ESFT) cell line SK-N-MC from betulinic acid induced
28 apoptosis by alpha-DL-tocopherol. *Toxicology Letters* 153: 201-212, 2004.
- 29 36. Hervouet E, Simonnet H, and Godinot C, Mitochondria and reactive oxygen species in
30 renal cancer. *Biochimie* 89:1080-1088, 2007.
- 31 37. Orrenius S, Gogvadze V, and Zhivotovsky B, Mitochondrial oxidative stress:
32 implications for cell death. *Annu.Rev.Pharmacol.Toxicol.* 47: 143-183, 2007.
- 33 38. Kiessling MK, Klemke CD, Kaminski MM, Galani IE, Krammer PH, and Gulow K,
34 Inhibition of constitutively activated nuclear factor-kappaB induces reactive oxygen
35 species- and iron-dependent cell death in cutaneous T-cell lymphoma. *Cancer Res.* 69:
36 2365-2374, 2009.
- 37 39. Galaris D, Skiada V, and Barbouti A, Redox signaling and cancer: the role of "labile"
38 iron. *Cancer Lett.* 266: 21-29, 2008.
- 39 40. Valko M, Rhodes CJ, Moncol J, Izakovic M, and Mazur M, Free radicals, metals and
40 antioxidants in oxidative stress-induced cancer. *Chem.Biol.Interact.* 160: 1-40, 2006.

- 1 41. Jin HO, Park IC, An S, Lee HC, Woo SH, Hong YJ, Lee SJ, Park MJ, Yoo DH, Rhee
2 CH, and Hong SI, Up-regulation of Bak and Bim via JNK downstream pathway in the
3 response to nitric oxide in human glioblastoma cells. *Journal of Cellular Physiology*
4 206: 477-486, 2006.
- 5
6 42. Lee HJ, Wang CJ, Kuo HC, Chou FP, Jean LF, and Tseng TH, Induction apoptosis of
7 luteolin in human hepatoma HepG2 cells involving mitochondria translocation of
8 Bax/Bak and activation of JNK. *Toxicology and Applied Pharmacology* 203: 124-131,
9 2005.
- 10
11 43. Yu J and Zhang L, The transcriptional targets of p53 in apoptosis control. *Biochemical*
12 *and Biophysical Research Communications* 331: 851-858, 2005.
- 13
14
15 44. Shih CM, Ko WC, Wu JS, Wei YH, Wang LF, Chang EE, Lo TY, Cheng HH, and
16 Chen CT, Mediating of caspase-independent apoptosis by cadmium through the
17 mitochondria-ROS pathway in MRC-5 fibroblasts. *Journal of Cellular Biochemistry*
18 91: 384-397, 2004.
- 19
20
21 45. Thayyullathil F, Chathoth S, Hago A, Patel M, and Galadari S, Rapid reactive oxygen
22 species (ROS) generation induced by curcumin leads to caspase-dependent and -
23 independent apoptosis in L929 cells. *Free Radic.Biol.Med.* 45: 1403-1412, 2008.
- 24
25
26 46. Kang YH, Yi MJ, Kim MJ, Park MT, Bae S, Kang CM, Cho CK, Park IC, Park MJ,
27 Rhee CH, Hong SI, Chung HY, Lee YS, and Lee SJ, Caspase-independent cell death
28 by arsenic trioxide in human cervical cancer cells: Reactive oxygen species-mediated
29 poly(ADP-ribose) polymerase-1 activation signals apoptosis-inducing factor release
30 from mitochondria. *Cancer Research* 64: 8960-8967, 2004.
- 31
32
33 47. Kim JS, Lee JH, Jeong WW, Choi DH, Cha HJ, Kim DH, Kwon JK, Park SE, Park
34 JH, Cho HR, Lee SH, Park SK, Lee BJ, Min YJ, and Park JW, Reactive oxygen
35 species-dependent EndoG release mediates cisplatin-induced caspase-independent
36 apoptosis in human head and neck squamous carcinoma cells. *International Journal of*
37 *Cancer* 122: 672-680, 2008.
- 38
39
40 48. Ganguly A, Das B, Roy A, Sen N, Dasgupta SB, Mukhopadhyay S, and Majumder
41 HK, Betulinic acid, a catalytic inhibitor of topoisomerase I, inhibits reactive oxygen
42 species-mediated apoptotic topoisomerase I-DNA cleavable complex formation in
43 prostate cancer cells but does not affect the process of cell death. *Cancer Res.* 67:
44 11848-11858, 2007.
- 45
46
47 49. Voehringer DW and Meyn RE, Redox aspects of Bcl-2 function.
48 *Antioxid.Redox.Signal.* 2: 537-550, 2000.
- 49
50
51 50. Tripathi P and Hildeman D, Sensitization of T cells to apoptosis - A role for ROS?
52 *Apoptosis* 9: 515-523, 2004.
- 53
54
55 51. Fernandez Y, Verhaegen M, Miller TP, Rush JL, Steiner P, Opipari AW, Jr., Lowe
56 SW, and Soengas MS, Differential regulation of noxa in normal melanocytes and
57 melanoma cells by proteasome inhibition: therapeutic implications. *Cancer Res.* 65:
58 6294-6304, 2005.
- 59
60
61
62
63
64
65

